Hardness and elastic properties of dehydrated cuticle from the lobster *Homarus americanus* obtained by nanoindentation

C. Sachs, H. Fabritius, and D. Raabe[a)]
Max-Planck-Institut für Eisenforschung, 40237 Düsseldorf, Germany

(Received 21 December 2005; accepted 2 March 2006)

The mechanical properties of biological materials are well adjusted to their function. An excellent example for such materials is the cuticle or exoskeleton of arthropods. In this study, dehydrated cuticle of the American lobster *Homarus americanus* was examined as a model for a mineralized biological composite material. Nanoindentation testing is a powerful method for revealing gradients and anisotropy in the hardness and the elastic properties of such materials. The air-dried test specimens stem from different parts of the crusher claw with different biological functions. Both the exocuticle and the endocuticle were probed in normal and in the transverse direction to the cuticle surface. For estimating variations in the grade of mineralization, the samples which were tested as cross-sections of the cuticle were analyzed by the use of energy dispersive x-ray mapping. The microstructure of fracture surfaces of the test specimens was investigated using scanning electron microscopy. Due to the use of dehydrated samples, our results do not reflect the exact properties of lobster cuticle in the natural hydrated state, but they can be regarded as a fairly good approximation to the in vivo state.

I. INTRODUCTION

A common principle in the design of structural biological materials like shells or bone is their hierarchical organization on all length scales. This principle is perfectly implemented in the cuticle forming the exoskeletons of Arthropoda or joint-limb animals, which include such groups as insects, crustaceans, and chelicerates. The cuticle represents a functional unit covering the whole body of the organisms and is locally modified to meet diverse requirements like providing mechanical support to the body, enabling motility through the formation of joints and attachment sites for muscles, and protecting against predators.[1,2] Crustacea represent an important class inside this phylum. Our model organism, the American lobster *Homarus americanus* is a large crustacean belonging to the taxon Decapoda.

The body of the lobster consists of two main parts, the cephalotorax and the abdomen (tail) (Fig. 1). The cephalothorax includes the cephalon (head) and the thorax (the mid-section or body), which are covered by a hard shell called the carapace. The thorax has five pairs of legs. The first pair have evolved into large claws referred to as crusher claw and pincher claw, according to their function. The crusher claw is used to crack the lobster's prey while the pincher claw is used to hold the prey. The remaining leg pairs are mainly used for walking and grooming.[3–6]

Like arthropod cuticles in general, the cuticle of the lobster *Homarus americanus* is a multilayered chitin-protein-based biological composite. Most crustaceans, including the lobster, additionally harden their cuticle by the incorporation of variable amounts of nanoscopic biomineral particles, in this case calcite and amorphous calcium carbonate (ACC).[7] Macroscopically, the cuticle consists of three structurally different layers, namely, epicuticle, exocuticle, and endocuticle (Fig. 2). The outermost epicuticle is a thin waxy layer, which provides a permeability barrier to the environment. The structure of the mechanically relevant exocuticle and endocuticle follows the principle of a twisted plywood structure also referred to as the classical Bouligand structure.[8,9]

The basic components of the cuticle are chitin-protein nanofibrils with diameters of about 2–5 nm and lengths of about 300 nm. They are composed of crystalline α-chitin, which is formed by the antiparallel arrangement of 18–25 chains of the polysaccharide chitin and are wrapped with proteins. These nanofibrils cluster to form chitin-protein fibers with diameters between 50 and 250 nm, which are subsequently arranged parallel to each other forming chitin-protein planes.[10] In the case of mineralized chitin-protein planes, the mineral particles are embedded between the chitin-protein nanofibrils.[11–13] The planes are stacked on top of each other and rotate

a)Address all correspondence to this author.
e-mail: raabe@mpie.de
DOI: 10.1557/JMR.2006.0241

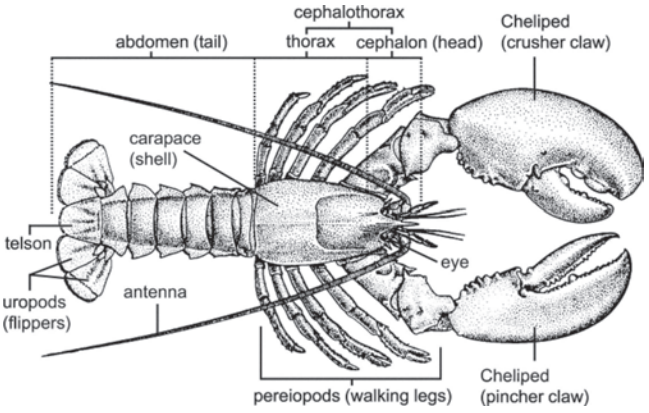

FIG. 1. Schematic drawing of the morphology of *Homarus americanus* according to Carpenter.[6]

gradually around their normal axis, which is equal to the normal axis of the cuticle surface. A stack of these superimposed planes that completes a rotation of 180° is referred to as one Bouligand or twisted plywood layer. Characteristic of the lobster cuticle is the presence of a well-developed pore canal system with numerous canals penetrating it perpendicular to the surface. The pore canals contain long, soft, and probably flexible tubes. The fibers of each chitin-protein plane are arranged around the lenticellate cavities of the pore canals generating a structure resembling a twisted honeycomb [Fig. 3(b)].[14]

The highly controlled composition and the hierarchical structure of the cuticle lead to well-defined mechanical properties.[3,15–21] Micro- and nanoindentation are particularly suitable for the identification of variations in the mechanical properties and thus have become established techniques in material testing. Depending on the applied load and the characteristic volume, mechanical properties of the material can be examined at different length scales and different levels of organization. The option for probing multiple positions in one measurement allows a systematic scanning of an area to detect variations in the local mechanical properties. Previous investigations of lobster cuticle using microindentation in the direction normal to the cuticle surface have revealed a sharp gradient in the hardness and the elastic properties from the exocuticle to the endocuticle.[22] However, due to the limited minimal load and the resulting indent size of the microindenter, testing of the approximately 200-μm-thick exocuticle was inapplicable in cross sections of the cuticle. To obtain data on hardness and elastic properties of the endocuticle as well as of the exocuticle both parallel and perpendicular to the surface, nanoindentation was used to test samples from three distinctive parts of the crusher claw.

II. MATERIAL AND METHODS

A. Sample preparation

The specimens used for nanoindentation were taken from the air-dried crusher claw of a large adult, nonmolting American lobster (*Homarus americanus*) bought from a local food supplier. Three locations were chosen as sampling points, the first [C1, Fig. 4(a)] and the second one [C2, Fig. 4(a)] were located on the upper surface of the claw (referred to as the "shell"), and the third one was taken from one of the large reinforced ridges used for crushing prey, which are located on the inner edge of the immobile finger of the claw [referred to as "tooth," C3 in Fig. 4(a)]. From each location, three samples were examined. Each of these samples was cleaved into four smaller pieces from which one was glued with its cross section pointing upward and two with their surface pointing upward to the sample holders. Flat magnetic steel disks with a diameter of 12 mm and a height of 3 mm were used as sample holders in combination with a two-component adhesive (UHU plus endfest 300, UHU GmbH, Brühl, Germany) for fixation [Fig. 4(b)].

Subsequently, the samples were knife polished using a rotary microtome (Leica RM 2165, Leica Microsystem GmbH, Wetzlar, Germany) equipped with a steel knife. The feed rate was gradually decreased from 10 μm down to 500 nm to obtain the lowest surface roughness possible. Before polishing, the epicuticle of the samples designated for indentation of the exocuticle in normal

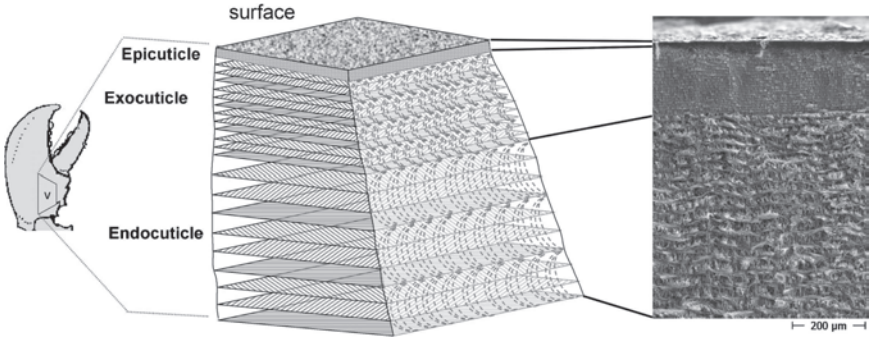

FIG. 2. Organization of the cuticle of *Homarus americanus*, schematic representation, and scanning electron micrograph of a cross section through the cuticle of a cheliped.

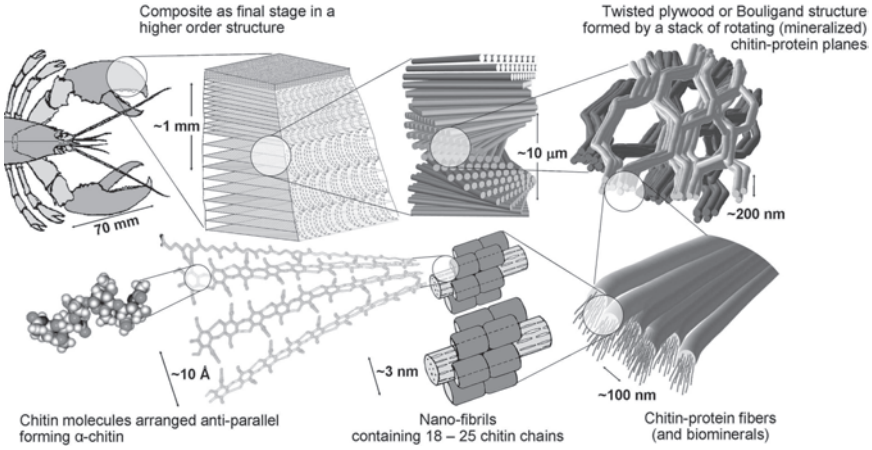

FIG. 3. Schematic representation of the hierarchical organization of the arthropod cuticle.

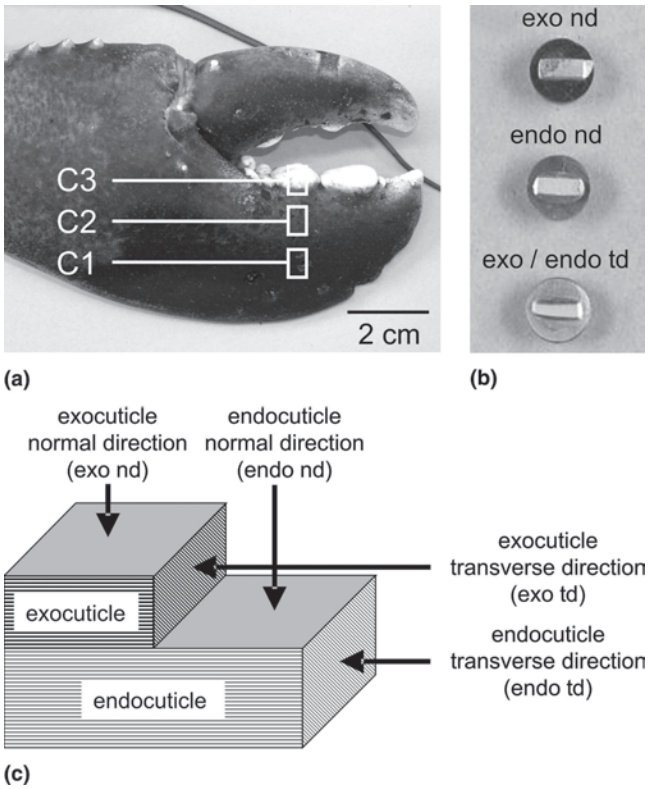

FIG. 4. Samples used for nano-indentation: (a) locations of the samples prepared from the crusher claw (C1, C2, C3); (b) test specimens exposing the polished surfaces of the exocuticle parallel to the cuticle surface (exo nd), the endocuticle parallel to the cuticle surface (endo nd), and exo and endocuticle in cross-section (exo/endo td), mounted on holders; and (c) schematic representation of the four different indentation sites [(nd) normal direction and (td) transverse direction].

direction was removed. The exocuticle of the samples designated for indentation of the endocuticle in normal direction was gradually removed with 20-µm-thick cuts until the desired depth was reached. After polishing, all samples were cleaned by washing them for 1 s in 100% methanol.

B. Nanoindentation

The nanoindentation tests were performed using a Hysitron Tribo-Indenter (Hysitron Inc., Minneapolis, MN) equipped with 1D-transducer enabling a maximum indentation force of up to 12 mN. For indenting, we used a Berkovich diamond tip. As a load function, a triangular and trapezoidal course was designed. The maximum load of 1000 µN was applied and removed at a rate of 200 µN/s. The holding time was defined as 0 or 20 s, respectively. The samples with their cross section pointing upward were indented in transverse direction both in the exo- and endocuticle, and the samples with their surface pointing upward were indented in the normal direction. On each indentation site, three quadratic patterns composed of 100 indents with a spacing of 5 µm were placed. The area function to obtain the contact area A_c was derived from measuring a polymethyl-methacrylate (PMMA) standard.

The reduced elastic modulus was calculated by the Oliver–Pharr method,[23] which is included in the Hysitron software (Triboview version 6.0.0.31). The contact stiffness S defined as the slope at the beginning of the unloading curve is given by

$$S = \frac{dP}{dH} \quad ,$$

where P is indentation load, and h is indentation depth. For determination, the initial (90–20%) unloading curve is fitted by a power law

$$P = A \times (h - h_f)^m \quad ,$$

where A and m are coefficients, and h_f final indentation depth. The elastic modulus E of the indented material is related to the contact stiffness by

$$S = \frac{2\beta}{\sqrt{\pi}} \times \left(\frac{1 - \nu^2}{E} + \frac{1 - \nu_i^2}{E_i} \right)^{-1} \times \sqrt{A_c} \quad ,$$

where ν_i is Poisson's ratio of the indenter, E_i is the elastic modulus of the indenter, and β is a constant for the

indenter geometry (1.034 for the Berkovich indenter). Consequently, the reduced elastic modulus E_{red} can be defined as

$$E_{red} = \frac{\sqrt{\pi}}{2\beta} \times \frac{S}{\sqrt{A_c}} \quad ,$$

and is linked to the elastic modulus E by

$$E_{red} = \frac{E}{1 - \nu^2} \quad ,$$

if the indenter is considered to be much stiffer than the probed material. Because Poisson's ratio of the cuticle in our area of interest is not satisfactory evaluated, we refer to the reduced elastic modulus as stiffness in the following discussion. The hardness is defined by

$$H = \frac{P_{max}}{A_c} \quad ,$$

where P_{max} is the maximal achieved loading force.

C. Microscopy and energy dispersive x-ray analysis

The remaining cleaved samples were prepared for scanning electron microscopy (SEM). The fractured surfaces were sputter-coated with 10 nm gold, mounted on aluminum sample holders, and examined in a CamScan 4 scanning electron microscope (Elektronen-Optik GmbH, Dortmund, Germany). The samples indented transversally into the cross-section were prepared for SEM using the same protocol. A qualitative energy dispersive x-ray (EDX) mapping for calcium was carried out at the interface between the endocuticle and the exocuticle using an Oxford EDX ISIS LINK system (Oxford Instruments, Buckinghamshire, UK).

D. Statistical analysis

The obtained hardness and stiffness data for the holding times 0 and 20 s and the values for the hardness and the reduced elastic modulus at the different indentation sites were tested for statistically significant differences employing one way analysis of variance (ANOVA) at $p < 0.05$ using the Origin 7.5 (OriginLab Corporation, Northampton, MA) software package.

III. RESULTS

A. Mechanical properties

The mechanical properties derived by nanoindentation are the hardness and the reduced elastic modulus. Each data point depicted in Figs. 5 and 6 represents the average of 300 indents, and the standard deviation is indicated by the scatter bars. The first two sets of data points represent the values for the exocuticle in normal and in transverse direction; the third and fourth represent the corresponding values for the endocuticle. For evaluating the time effect on hardness (Table I, Fig. 5) and reduced elastic modulus (Table II, Fig. 6), the values for a holding time of 0 and 20 s are added to the diagrams. A holding time of 20 s apparently leads to a decrease of the measured values for the hardness and the reduced elastic modulus with several values being significantly smaller for this holding time (Figs. 5 and 6). Due to the longer holding time at maximum load, the indenter can interact with the probed volume before unloading, which allows relaxation processes to take place. This convergence to a closer equilibrium state results in slightly more stable values and reduced variance. Hence the values for the hardness and the reduced elastic modulus with a holding time of 20 s will be used in the following description of the results and the discussion.

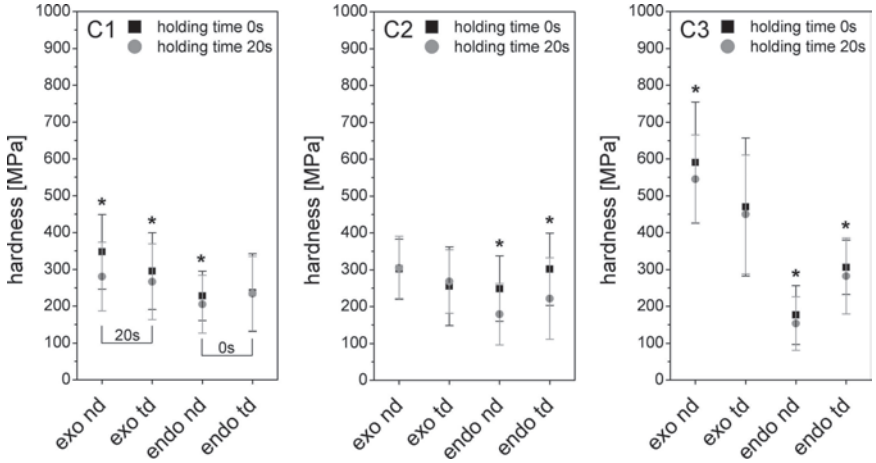

FIG. 5. Hardness depending on the indentation site at an applied maximum load of 1000 μN (C1 to C3). The first pair of data points represents the values for the exocuticle in normal (exo nd) and in transverse direction (exo td); the second pair represents the value for the endocuticle (endo nd) in normal and in transverse direction (endo td). The data sets marked with an asterisk (*) indicate significant differences ($p < 0.05$) between the values for a holding time of 0 and 20 s. The brackets mark data sets that are not significantly different ($p = 0.089$ for C1 comparing exo nd to exo td for a holding time of 20 s and $p = 0.222$ for C1 comparing endo nd to endo td for a holding time of 0 s).

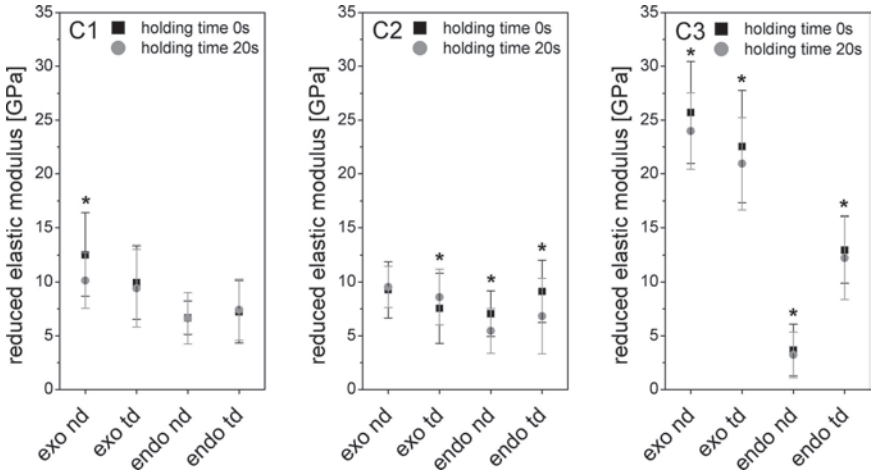

FIG. 6. Reduced elastic modulus depending on the indentation site at an applied maximum load of 1000 μN (C1 to C3). The first pair of data points represents the values for the exocuticle in normal (exo nd) and in transverse direction (exo td); the second pair represents the value for the endocuticle (endo nd) in the normal direction and in the transverse direction (endo td). The data sets marked with an asterisk (*) indicate significant differences ($p < 0.05$) between the values for holding times of 0 and 20 s.

TABLE I. Comparison of average hardness values for different holding times (0 or 20 s) obtained for samples C1, C2, and C3.

	Hardness exocuticle (MPa)				Hardness endocuticle (MPa)			
	Normal direction		Transverse direction		Normal direction		Transverse direction	
Sample	0 s	20 s	0 s	20 s	0 s	20 s	0 s	20 s
C1 shell	347	280	295	266	228	205	237	234
C2 shell	302	305	255	268	249	179	301	222
C3 tooth	590	545	470	450	176	154	306	282

TABLE II. Comparison of average reduced elastic modulus (referred to as stiffness in the discussion) for different holding times (0 s or 20 s) obtained for samples C1, C2, and C3.

	Reduced elastic modulus exocuticle (GPa)				Reduced elastic modulus endocuticle (GPa)			
	Normal direction		Transverse direction		Normal direction		Transverse direction	
Sample	0 s	20 s	0 s	20 s	0 s	20 s	0 s	20 s
C1 shell	12.5	10.1	9.9	9.4	6.7	6.6	7.2	7.4
C2 shell	9.3	9.5	7.6	8.6	7.1	5.4	9.1	6.8
C3 tooth	25.7	24.0	22.5	21.0	3.7	3.2	13.0	12.2

The hardness data as a function of indentation site and holding time are shown in Fig. 5. The samples C1 and C2 (shell) achieved a maximum hardness of 280 and 305 MPa in the exocuticle probed in normal direction compared to a maximum hardness of 545 MPa of the sample C3 (tooth) for the same indentation site. By changing the indentation site in the exocuticle to the transverse direction, the hardness decreases to 266 and 268 MPa for the samples C1 and C2 and to 450 MPa for the sample C3, which is equal to a difference of 14 MPa (C1), 37 MPa (C2), and 140 MPa (C3). In normal direction of the endocuticle the hardness reaches values of 205 MPa (C1), 179 MPa (C2), and 154 MPa (C3). However, in the endocuticle, the maximum hardness is reached in the transverse direction. It amounts to 234 and 222 MPa for the samples C1 and C2 (shell) and to 282 MPa for the sample C3 (tooth). Consequently, the gradient from the exocuticle to the endocuticle is more pronounced in the normal direction than in the transverse direction. In normal direction, it is on the order of 75 and 126 MPa for the samples C1 and C2 and 391 MPa for the sample C3. In the transverse direction, it amounts to 32 and 46 MPa for samples C1 and C2 or to 168 MPa for the sample C3, respectively.

Accordingly, the reduced elastic modulus as a function of indentation site and holding time is shown in Fig. 6. In the exocuticle, samples C1 and C2 (shell) reached a maximum reduced elastic modulus of 10.1 and 9.5 GPa in normal direction. Here the sample C3 (tooth) obtains a maximum of 24 GPa. In the corresponding transverse direction, the reduced modulus decreases to 9.4 and 8.6 GPa for samples C1 and C2 and to 21 GPa for sample C3, which is equal to a difference of 0.7, 0.9, and 3.0 GPa, respectively. In the endocuticle the reduced modulus in the normal direction reaches values of 6.6 and 5.4 GPa for samples C1 and C2, and a lower one of 3.2 GPa for sample C3. Analogous to the hardness, in the endocuticle the maximum reduced modulus is detected in transverse direction. It amounts to 7.4 and 6.8 GPa for samples C1 and C2 (shell) and to 12.2 GPa for sample C3 (tooth). Like the hardness, the gradient from the exocuticle to the endocuticle is more pronounced in the normal direction than in the transverse direction. In the normal direction, it is on the order of 3.5 and 4.1 GPa for samples C1 and C2 and 20.8 GPa for sample C3. In the

transverse direction, it amounts to only 2.0 and 1.8 GPa for samples C1 and C2 or to 8.8 GPa for sample C3.

B. Microstructure and mineralization

The scanning electron microscopic overview image of the perpendicularly fractured cuticle from the upper surface of the claw (shell, samples C1 and C2) shows the differences in the microstructure of the outer exocuticle and the inner endocuticle [Fig. 7(a)]. The interface between them is easily distinguishable as a change in the stacking density of the Bouligand layers. In the exocuticle, the stacked fiber layers take about 10 μm to complete a 180° rotation, and in the endocuticle, about 30 μm. The exocuticle is about 200 μm thick in the C1 and C2 areas. In the sample taken from the reinforced ridges used for crushing prey, which are located on the inner edge of the claw (tooth, sample C3) the endocuticle easily reaches thicknesses of up to 1.5 mm [Fig. 7(b)]. The stacking density of the rotating fiber planes does not differ from the shell samples. At higher magnifications, details of the microstructure become visible. In the exocuticle [Fig. 7(c)], the mineralized fibers are more densely packed, and the pore canals are smaller than in the endocuticle [Fig. 7(d)].

After the indentation experiments, EDX mapping was conducted on the samples where the cross-section had been tested. To detect possible differences in the grade of mineralization of the different layers, the interface between exocuticle and endocuticle was chosen as the area of interest. The results of the qualitative analysis for calcium content are shown in Fig. 8. The exocuticle-endocuticle interface can be seen as change in the shading in the center of the images for all three samples. In all three samples, the calcium count rate is higher in the exocuticle than in the endocuticle. While the difference is less pronounced for the samples C1 and C2 (shell), the sample C3 (tooth) shows a more pronounced gradient of calcium counts from exo- to endocuticle.

IV. DISCUSSION

Biological materials display sophisticated designs to fulfill diverse requirements. These designs are realized through the control of the local structure and composition and, therefore, of the mechanical properties of the materials. As our samples were prepared in a dehydrated state, our results do not reflect the actual mechanical properties of the cuticle in the living lobster. *In vivo*, arthropod cuticles are always hydrated and the grade of hydration plays an important role in their mechanical properties since water is known to act as a plastifier in such materials.[17] Therefore, hardness and stiffness of lobster cuticle in its natural state are going to be lower than the

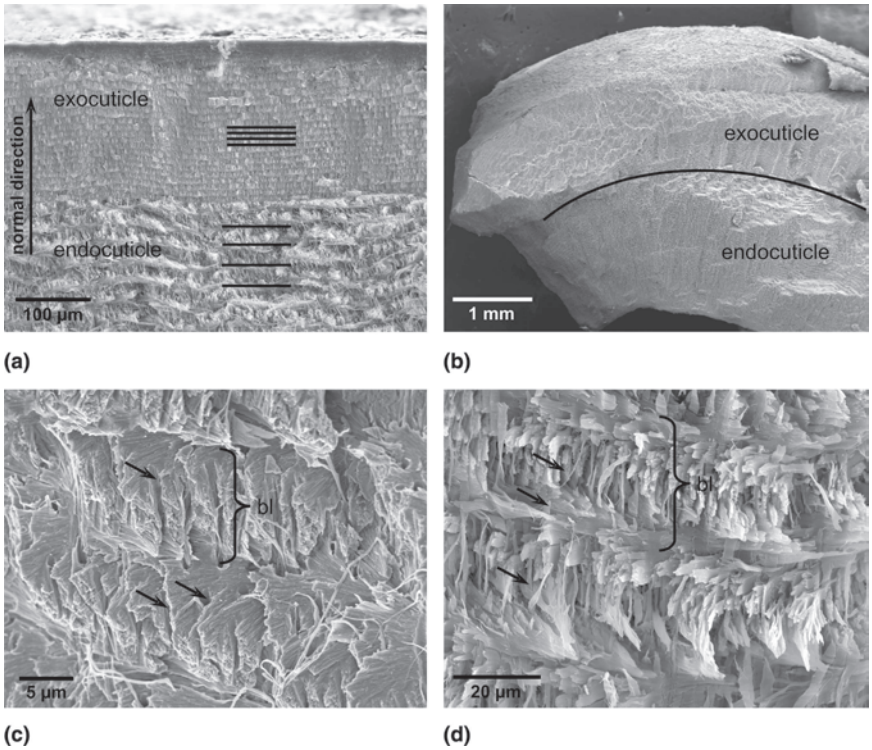

FIG. 7. Microstructure of the cuticle: (a) sample of shell cuticle (C1) fractured perpendicular to the cuticle surface; lines mark the stacks of twisted plywood layers. (b) Overview of the fractured cuticle of the crushing ridge (C3, tooth); the line on the fracture surface marks the interface between exo- and endocuticle. (c) Detail image of fractured exocuticle, bl Bouligand layer; arrows mark the pore canals. (d) Detail image of fractured endocuticle, bl Bouligand layer; arrows mark the pore canals.

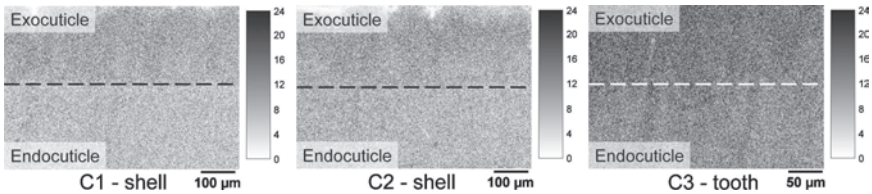

FIG. 8. Qualitative EDX mapping of calcium at the interface between exocuticle and endocuticle; C1 and C2 are the samples from the shell and C3 is the sample from the tooth structure. The dashed line marks the interface between exocuticle and endocuticle; the grayscale codes represent the registered calcium counts.

values we present for dehydrated cuticle. Nevertheless, the gradients and the anisotropy found in dry material are unlikely to differ significantly from hydrated material assuming that the effect of hydration is approximately homogeneous throughout the cuticle. This is also supported by the fact that the cuticle of the lobster is heavily mineralized and the mechanical properties of mineralized cuticles are dominated by the minerals.[17] To estimate the influence of hydration, a comparison of hardness and stiffness in the dry and the wet state is necessary. Our attempts on performing nanoindentation on freshly extracted cuticle in its natural hydrated state did not deliver feasible results because of desiccation effects occurring in the samples during knife polishing of the indentation sites and during the testing. This is a major problem because the indentation depth is below 1 μm, a distance where desiccation proceeds very fast and can hardly be controlled. Performing the experiments in water, physiological solutions, or in a controlled atmosphere can result in swelling as well as local demineralization effects, which would also affect the results. Preliminary experiments using fresh samples covered with a thin film of Vaseline to prevent desiccation could not be evaluated due to irreproducible interactions of the Vaseline with the indenter tip. These problems could probably be overcome by further refining the sample preparation or by using other methods of mechanical testing like tensile or bending tests where larger sample volumes are investigated. These tests make it much easier to keep the discrepancy between the natural state and the actual state during testing of the material to a minimum.

With exo- and endocuticle, the cuticle of the American lobster *Homarus americanus* is composed of two mechanically relevant layers that show different characteristics in their mechanical properties.[22] In the crusher claw, the outer exocuticle is structurally modified in the two different areas investigated in this study. The cuticle taken from the shell in the locations C1 and C2 [Fig. 4(a)] performs the role of structural support for the exoskeleton, and the cuticle taken from the reinforced ridge on the inner edge of the immobile finger of the claw [tooth region, C3, Fig. 4(a)] performs a specific function, namely crushing the prey of the lobster, mostly hard shelled mollusks. In the shell, the exocuticle has a continuous thickness of approximately 200 μm. In the tooth area, the exocuticle is enlarged to a thickness of more than 1 mm. A comparison of the hardness determined in normal direction shows that with 545 MPa, the exocuticle of the tooth is almost twice as hard as the exocuticle of the shell with 280 MPa (C1) or 305 MPa (C2) (Table I). In the transverse direction, the hardness decreases about 5% to 266 MPa (C1, not significant) or about 12% to 268 MPa (C2) in the shell and about 17% to 450 MPa (C3) in the tooth. Regarding the stiffness of the exocuticle, a similar trend can be observed. The stiffness of tooth amounts to 24.0 GPa in the normal direction and 21.0 GPa in the transverse direction, which is more than twice as high as the stiffness of the shell, which reaches values of 10.1 GPa in the normal direction and 9.4 GPa in the transverse directions for the sample C1 as well as 9.5 GPa in the normal direction and 8.6 GPa in the transverse directions for the sample C2 (Table II). As for the hardness, the maximal stiffness is obtained in the normal direction.

In the endocuticle, the hardness varies less within the tested samples. In the normal direction, the hardness of the samples reaches values of 205 MPa (C1), 179 MPa (C2), and 154 MPa (C3) (Table I). The hardness values determined in the transverse direction of the endocuticle amount to 234 MPa (C1) and 222 MPa (C2) in the shell and 282 MPa (C3) in the tooth. Regarding the stiffness of the endocuticle, the determined values in the normal direction are 6.6 GPa (C1) and 5.4 GPa (C2) in the shell and 3.2 GPa (C3) in the tooth. In the transverse direction, the stiffness of the shell amounts to 7.4 GPa (C1) and 6.8 GPa (C2), and that of the tooth to 12.6 GPa (C3) (Table II). It should be noted that in the endocuticle, the maximal hardness and stiffness are observed in the transverse direction, which is opposite of what occurs in the exocuticle. This orientation dependence of the properties shows that there is a pronounced anisotropy in both layers of the material.

Regarding the layer-specific anisotropy of hardness and stiffness, the pronounced fiber texture of the cuticle[21] can induce this effect if different mechanical properties are assumed for the fibers in their longitudinal and transverse axis. In the case of lobster cuticle, probed in normal direction, the mechanical response is limited to the properties of the fibers in their transverse axis. Probing in the transverse direction of the cuticle, the

properties of the fibers in both their longitudinal and transverse axis contribute to the mechanical response due to the rotation of the fibers around the normal direction of the cuticle, the size of the indents, and the extension and distribution of the indentation patterns. In the case of our chitin-protein fibers with embedded calcium carbonate crystallites, one may assume that they resist mechanical loads better in the longitudinal axis than they do in the transversal axis. This is a possible explanation for why hardness and stiffness of the endocuticle are higher in the transverse direction. However, the orientation of the fibers cannot explain why hardness and stiffness of the exocuticle display opposite behavior. Because of the higher stacking density in the exocuticle, the indenter interacts with a volume of the sample where the fiber planes rotate in higher angles around the normal direction of the cuticle and thus complete a rotation of 180° over a distance smaller than in the endocuticle. This higher rotation density of the material together with the higher grade of mineralization indicated by the EDX analysis might outweigh the influence of the fiber texture on the mechanical properties of the exocuticle. Similar anisotropic behavior due to fiber orientation was before observed in human bone.[24]

A comparison of the hardness and stiffness obtained for all samples reveals a pronounced gradient of these properties from the exocuticle to the endocuticle. Particularly in the tooth, the hardness decreases about 72% in the normal direction and 37% in the transverse direction along with a reduction of the stiffness about 87% in the normal direction and 42% in the transverse direction. In the shell, the hardness changes 27% (C1) and 41% (C2) in the normal direction and 12% (C1) and 17% (C2) in the transverse direction from the exocuticle to the endocuticle. The stiffness amounts to 35% (C1) and 43% (C2) less in the normal direction and 21% (C1) and 21% (C2) in the transverse direction from the exocuticle to the endocuticle. The distinct variations in hardness and stiffness between exocuticle and endocuticle of all investigated samples can be explained by a different grade of mineralization and the different stacking density of the Bouligand layers. The comparison between the microstructure of the exocuticle and the endocuticle shows that the stacking density in the exocuticle is three times higher than that in the endocuticle. Additionally, the EDX mappings reveal a strong and sharp gradient in the calcium content between the exo- and endocuticle. Qualitative EDX mapping for calcium can be used as an indication for the grade of mineralization.

While hardness and stiffness of the endocuticle do not vary greatly between the samples from the two different locations, there are, however, distinct variations in these properties in the exocuticle of samples from the shell and the tooth. The hardness and stiffness of the tooth exocuticle are much higher than the values determined for shell exocuticle. This corresponds well with the different biological functions of the exoskeleton in the two investigated areas. The special function of the tooth as a crushing tool certainly requires higher hardness and wear resistance than the cuticle in the shell areas, which has only structural function. This task is accomplished through a much higher grade of mineralization in the tooth as indicated by the qualitative EDX mappings (Fig. 8). A similar adaptation of the cuticle to a specific function has been shown before for the smashing limb of the mantid shrimp *Gonodactylus*, where the cuticle becomes harder and increasingly mineralized toward the outside, which is used to smash hard-shelled prey.[25]

V. CONCLUSIONS

In this study, we examined the mechanical properties of dehydrated exocuticle and endocuticle from the claws of the lobster *Homarus americanus* by employing nanoindentation. To detect anisotropy and gradients in the cuticle, different indentation sites were chosen. Although the obtained values for hardness and thickness of the material are undoubtedly higher than those for cuticle in the natural hydrated state it is unlikely that the gradients and anisotropy differ greatly due to the presumably uniform effect of hydration and the high grade of mineralization of lobster cuticle. The SEM and qualitative EDX examinations revealed several factors influencing hardness and stiffness. The stacking density of the Bouligand layers leads to an increase of the hardness and stiffness from the endocuticle to the exocuticle. This gradient is further affected by the grade of mineralization. In the case of the specialized reinforced ridges used for crushing (tooth), the exocuticle is almost twice as hard and stiff as the exocuticle of the neighboring claw parts (shell). The interface between the exocuticle and the endocuticle is well defined by a change in the stacking density and the grade of mineralization.

Due to the pronounced fiber texture, a distinct anisotropy of the mechanical properties emerges in the endocuticle, which results in maximum hardness and stiffness in the transverse direction. In contrast, the maximum hardness and stiffness in the exocuticle were observed in the normal direction. The higher stacking density of the twisted plywood layers and the increased grade of mineralization in the exocuticle might lead to different mechanical properties and outweigh the influence of the fiber texture.

ACKNOWLEDGMENT

The authors gratefully acknowledge the financial support from the Gottfried–Wilhelm–Leibniz program of the Deutsche Forschungsgemeinschaft (German Research Foundation).

REFERENCES

1. J.F.V. Vincent and J.D. Currey: *Mechanical Properties of Biological Materials* (Society for Experimental Biology, Cambridge, UK, 1980).
2. M.F. Ashby and U.G.K. Wegst: The mechanical efficiency of natural materials. *Philos. Mag.* **84,** 2167 (2004).
3. D.F. Travis: Structural features of mineralization from tissue to macromolecular levels of organization in the decapod Crustacea. *Ann. N.Y. Acad. Sci.* **109,** 177 (1963).
4. F.J. Vernberg and W.B. Vernberg: *The Biology of Crustacea* (Academic Press, New York, 1983).
5. M.N. Horst and J.A. Freeman: *The Crustacean Integument: Morphology and Biochemistry* (CRC Press, Ann Arbor, MI, 1993).
6. K.E. Carpenter: *The Living Marine Resources of the Western Central Atlantic,* Vol. 1: Introduction, Molluscs, Crustaceans, Hagfishes, Sharks, Batoid Fishes, and Chimaeras. FAO Species Identification Guide for Fishery Purposes (American Society of Ichthyologists and Herpetologists Special Publication No. **5**, Food and Agriculture Organization of the United Nations, Rome, 2002), pp. 1–600.
7. F.C. Meldrum: Calcium carbonate in biomineralisation and biomimetic chemistry. *Int. Mater. Rev.* **48,** 187 (2003).
8. Y. Bouligand: Ultrastructural aspects of the calcification in crabs, in *7th Int. Congress of Electron Microscopy* **3,** (Grenoble, France, 1970), p. 105–106.
9. M-M. Giraud-Guille: Plywood structures in nature. *Curr. Opin. Solid State Mater. Sci.* **3,** 221 (1998).
10. M-M. Giraud-Guille: Chitin crystals in arthropod cuticles revealed by diffraction contrast transmission electron microscopy. *J. Struct. Biol.* **103,** 232 (1990).
11. R.D. Roer and R.M. Dillaman: The structure and calcification of the crustacean cuticle. *Am. Zool.* **24,** 893 (1984).
12. M-M. Giraud-Guille and Y. Bouligand: Crystal growth in a chitin matrix: The study of calcite development in the crab cuticle, in *Chitin World,* edited by Z.S. Karnicki, M.M. Brzeski, P.J. Bykowski, and A. Wojtasz-Pajak (Wirtschaftsverlag NW, Bremerhaven, Germany, 1995), pp. 136–144.
13. F. Manoli, S. Koutsopoulos, and E. Dalas: Crystallization of calcite on chitin. *J. Cryst. Growth* **182,** 116 (1997).
14. D. Raabe, P. Romano, C. Sachs, A. Al-Sawalmih, H-G. Brokmeier, S-B. Yi, G. Servos, and H.G. Hartwig: Discovery of a honeycomb structure in the twisted plywood patterns of fibrous biological nanocomposite tissue. *J. Cryst. Growth* **283,** 1 (2005).
15. N.F. Hadley: The arthropod cuticle. *Sci. Am.* **255,** 104–112 (1986).
16. J.F.V. Vincent: *Structural Biomaterials* (Princeton University Press, Princeton, NJ, 1990).
17. J.F.V. Vincent: Arthropod cuticle: A natural composite shell system. *Composites Part A* **33,** 1311 (2002).
18. A.C. Neville: *Biology of Fibrous Composites* (Cambridge University Press, Cambridge, UK, 1993).
19. J.F.V. Vincent and U.G.K. Wegst: Design and mechanical properties of insect cuticle. *Arthropod Struct. Dev.* **33,** 187 (2004).
20. D. Raabe, A. Al-Sawalmih, P. Romano, C. Sachs, H-G. Brokmeier, S-B. Yi, G. Servos, and H.G. Hartwig: Structure and crystallographic texture of arthropod bio-composites, in *Proc. 14th Int. Conf. Text. Mater. ICOTOM* **14**, 1665 (2005).
21. D. Raabe, P. Romano, C. Sachs, H. Fabritius, A. Al-Sawalmih, S-B. Yi, G. Servos, and H.G. Hartwig: Microstructure and crystallographic texture of the chitin-protein network in the biological composite material of the exoskeleton of the lobster *Homarus americanus. Mater. Sci. Eng., A* **421,** 143–153 (2006).
22. D. Raabe, C. Sachs, and P. Romano: The crustacean exoskeleton as an example of a structurally and mechanically graded biological nanocomposite material. *Acta Mater.* **53,** 4281 (2005).
23. W.C. Oliver and G.M. Pharr: An improved technique for determining the hardness and elastic modulus using the load and displacement sensing indentation experiments. *J. Mater. Res.* **7,** 1564 (1992).
24. Z. Fan, J.G. Swadener, J.Y. Rho, M.E. Roy, and G.M. Pharr: Anisotropic properties of human tibial cortical bone as measured by nanoindentation. *J. Orthop. Res.* **20,** 806 (2002).
25. J.D. Currey, A. Nash, and W. Bonfield: Calcified cuticle in the stomatopod smashing limb. *J. Mater. Sci.* **17,** 1939 (1982).